

OPEN

# Comparative Evaluation of the Effectiveness of Novel Hyaluronic Acid-Polynucleotide Complex Dermal Filler

Jong Hwan Kim<sup>1,4</sup>, Tae-Rin Kwon<sup>1,4</sup>, Sung Eun Lee<sup>1,2</sup>, Yoo Na Jang<sup>1,2</sup>, Hye Sung Han<sup>1,2</sup>, Seog Kyun Mun<sup>3</sup> & Beom Joon Kim<sup>1,2\*</sup>

HA (Hyaluronic acid) filler, the most commonly used dermal filler, causes several side effects. HA-PN (Hyaluronic acid-Polynucleotide), a new composite filler, has excellent biocompatibility and induces tissue regeneration. In this study, we compare the efficacies and safety profiles of these fillers. The characteristics of HA and HA-PN fillers were compared using scanning electron microscopy and rheometry. No morphological difference was noted between the fillers. However, the latter had higher viscosity and elasticity values. The HA-PN filler induced higher cell migration than the HA filler in a wound healing assay. It was also found to stimulate better collagen synthesis in human and mouse fibroblasts. The HA and HA-PN fillers were injected into SKH1 hairless mice to determine changes in their volume for up to 24 weeks. Increased cell migration and collagen synthesis were observed in mice injected with the HA-PN complex filler. Although the safety and durability of the HA and HA-PN fillers were similar, the latter induced a lower transient receptor potential vanilloid 4 expression and caused less stimulation upon injection. In conclusion, HA-PN complex fillers can stimulate fibroblast growth and facilitate volume growth and skin regeneration.

Dermal fillers can be used in simple and short procedures in surgery and rapid facial rejuvenation. There is growing interest in the use of fillers for tissue enlargement and improvement of skin aesthetic beauty<sup>1-3</sup>.

Synthetic facial fillers are composed of a biosynthetic polymer in combination with different injectable carriers, including hydrogels, beads, and liquids<sup>4</sup>. The most popular type of filler contains hyaluronic acid (HA). However, the use of HA fillers carries an inherent risk of hypersensitivity reactions because these fillers contain hyaluronan-related proteins and 1,4-butanediol diglycidyl ether (BDDE)<sup>5,6</sup>. In addition, small fragments of HA can cause inflammation and elicit adverse effects that include erythema, slight oedema, hematoma, itching, and pain<sup>7-9</sup>. A recent study showed that the biocompatibility of HA-based materials decreases with an increase in the number of modifications to this polysaccharide<sup>5,6,10</sup>.

Various dermal fillers have been developed to overcome the adverse effects accompanying the use of HA fillers<sup>6,11-14</sup>. Recently, a new filler product was synthesised using a purified polynucleotide (PN) extracted from salmon and other fish germ cells. This product is currently in use in Europe<sup>15</sup>. While existing filler products work by simply filling spaces in the skin<sup>16</sup>, PN-containing products also induce the regeneration of damaged tissues to result in a more natural tissue regeneration<sup>15</sup>. In addition, it has been reported that nucleotides promote the growth of human corneal fibroblasts and increase their remnants in ultraviolet B-damaged skin fibroblasts<sup>17</sup>. *In vitro* studies have demonstrated the therapeutic efficacy of polynucleotides in patients who received treatment for skin ectopia and have shown that polynucleotides promote rapid corneal epithelialisation after photorefractive keratectomy<sup>18,19</sup>.

The use of a PN filler offers the advantages of skin elasticity, collagen synthesis, and regeneration by stimulation of fibre elasticity. However, the volumising effect and durability of PN dermal fillers are not as good as those of existing dermal fillers<sup>15,20,21</sup>. In this study, we used an HA-PN (Hyaluronic acid-Polynucleotide) complex filler,

<sup>1</sup>Department of Dermatology, Chung-Ang University College of Medicine, Seoul, Korea. <sup>2</sup>Department of Medicine, Graduate School, Chung-Ang University, Seoul, Korea. <sup>3</sup>Department of Otorhinolaryngology-Head and Neck Surgery, Chung-Ang University College of Medicine, Seoul, Korea. <sup>4</sup>These authors contributed equally: Jong Hwan Kim and Tae Rin Kwon. \*email: [beomjoon@unitel.co.kr](mailto:beomjoon@unitel.co.kr)

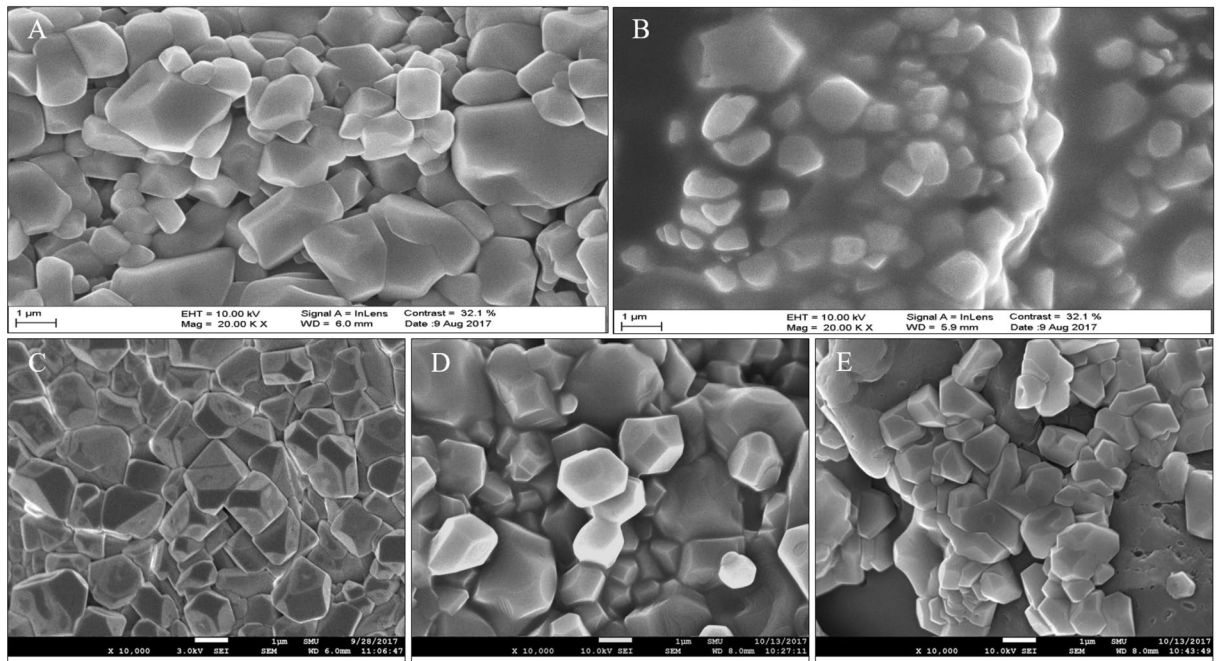


**Figure 1.** SEM images of HA and HA–PN fillers. (A) HA filler, Juvéderm VOLUMA. (B) HA filler, Juvéderm VOLBELLA. (C) HA–PN (0.1%) complex filler. (D) HA–PN (0.5%) complex filler. (E) HA–PN (1%) complex filler.

	$G'$ (Pa)	$G''$ (Pa)	$G^*$ (Pa)	$\delta$ ( $^\circ$ )
Juvederm VOLUMA <sup>®</sup>	$340.97 \pm 27.66$	$37.63 \pm 5.25$	$343.12 \pm 27.28$	$6.36 \pm 1.19$
Juvederm VOLBELLA <sup>®</sup>	$196.10 \pm 24.82$	$32.91 \pm 3.15$	$198.93 \pm 24.36$	$9.69 \pm 1.73$
HA-PN 0.1%	$1107.15 \pm 281.26$	$448.64 \pm 42.64$	$1197.48 \pm 271.95$	$22.84 \pm 3.80$
HA-PN 0.5%	$1165.65 \pm 237.13$	$323.56 \pm 26.58$	$1210.48 \pm 234.30$	$15.88 \pm 2.06$
HA-PN 1%	$509.66 \pm 87.55$	$132.56 \pm 21.92$	$526.63 \pm 90.17$	$14.59 \pm 0.42$

**Table 1.** Storage modulus ( $G'$ ), loss modulus ( $G''$ ), complex viscosity ( $\eta^*$ ), and phase angle ( $\delta$ ) measured at a frequency of 1 Hz at 25°C.

which has the advantages of both tissue regeneration and durability. This filler overcomes the disadvantages of its individual components. This study also aimed to demonstrate the commercial feasibility of the HA–PN complex filler by comparing the efficacies and safety profiles of HA and HA–PN complex fillers *in vitro* and *in vivo*.

## Results

**Scanning electron microscopy (SEM) analysis of HA and HA–PN complex fillers.** The morphologies of HA and HA–PN complex fillers were compared using SEM. Based on the SEM images, both fillers are made up of irregular and small polygonal particles (Fig. 1).

**Comparison of rheological properties of HA and HA–PN fillers.** The  $G'$  mean values of elasticity,  $G''$  mean values of viscosity,  $G^*$  mean values of viscoelasticity, and the mean values of  $\tan \delta$ , indicating the ratio of viscosity to elasticity, were measured (Supplementary Fig. 1, Table 1). All values were higher for the HA–PN complex fillers than for the HA fillers. These results confirmed that the addition of PN to HA increases the filler's elasticity, viscosity, viscoelasticity, and modulus of elasticity.

**Comparison of cell cytotoxicity and proliferation induced by HA, PN, and HA–PN treatments.** To assess the cytotoxic effects of HA, PN, and HA–PN treatments on human dermal fibroblast (HDF) and mouse fibroblast (L929) cells, comparative cytotoxicity tests using the MTT (3-(4, 5-dimethylthiazolyl-2)-2, 5-diphenyltetrazolium bromide) assay were performed. The cells were incubated with the fillers for 24 and 72 h before cytotoxicity was assessed (Fig. 2). HA, PN, and HA–PN did not display dose- or time-dependent cytotoxic effects. On the contrary, the proliferation of HDF cells was evident following treatment with only 1% PN, a combination of 0.1% HA and 0.5% PN, and a combination of 0.1% HA and 1% PN. Additionally, the proliferation of L929 cells increased significantly after treatment with a combination of 0.1% HA and 0.5% PN and a combination of 0.1% HA and 1% PN. In particular, co-treatment with 0.1% HA and 1% PN increased the proliferation of HDF and L929 cells by approximately 20%.

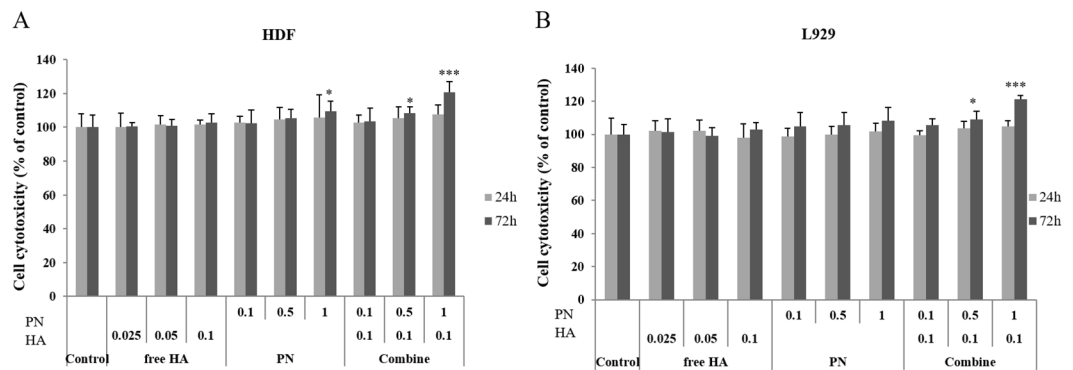


**Figure 2.** MTT assay to determine the viability of (A) HDF cells and (B) L929 cells after treatment with increasing concentrations of HA, PN, and HA–PN fillers for 24 h and 72 h. Statistical significance was determined by the Student's *t*-test. \**P* < 0.05, \*\**P* < 0.005, \*\*\**P* < 0.0005.

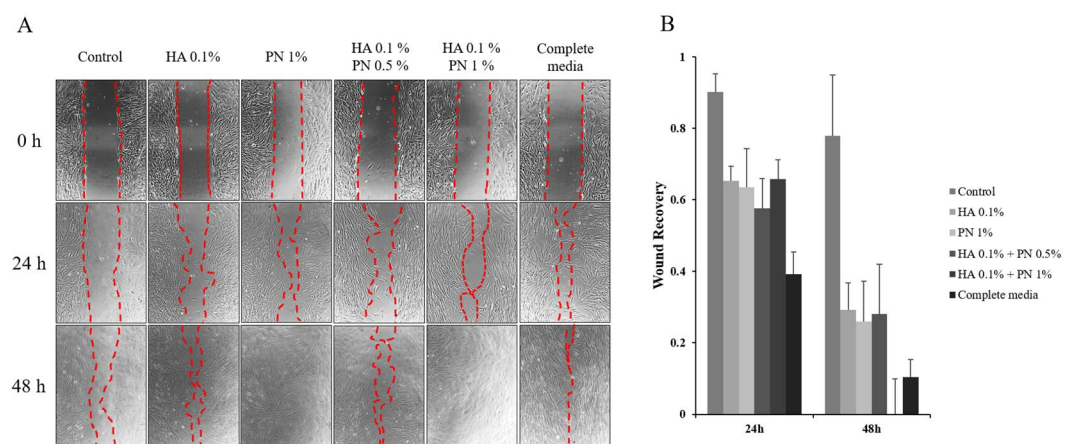


**Figure 3.** Effect of PN on the migration of human fibroblast cells. Wound Healing Analysis Images (Zoomth increasing concentrations of Ibidi chambers and cultured to near confluence. A free ‘scratch’ or wound was created on the bound monolayer of cultured cells. The cells were incubated in medium containing 0.1% HA, 0.5% PN, or 1% PN for 0, 24 and 72 h at 37 °C in a humidified incubator with a 5% CO<sub>2</sub> atmosphere. Medium Supplemented with 10% FBS was used in the complete medium group. The wound areas were quantified and expressed as a percentage of the initial wound area.

**Comparison of cell migration following HA, PN, and HA–PN treatment.** To further investigate the effects of HA, PN, and HA–PN on the proliferation of HDFs, a wound healing assay was performed after HA, PN, and HA–PN treatments. After incubation for 48 h, cell migration was confirmed (Fig. 3A). In particular, co-treatment with 0.1% HA and 0.5% PN showed the highest cell growth potential (Fig. 3B). These results suggest that PN is effective for cell proliferation.

**Comparison of collagen synthesis by HA, PN, and HA–PN treatments.** To determine the correlation between proliferative capacity and collagen expression, the expression of type I collagen at the protein level was analysed by western blotting using HDF cells treated with HA, PN, or HA–PN. Collagen expression was higher in the 0.5% PN group and the 0.1% HA and 0.5% or 1% PN co-treatment groups when compared to that in untreated HDF cells (Fig. 4A,B). Soluble collagen in cell culture supernatants was quantified using the Sircol collagen assay. A dose-dependent increase in collagen synthesis was observed in the PN group and the HA–PN co-treatment group, but not in the HA group (Fig. 4C). Therefore, PN treatment induced an increase in collagen synthesis in the cells.

**Comparison of durability between HA and HA–PN complex fillers *in vivo*.** To confirm the durabilities of the HA and HA–PN fillers, 100 μL of each filler was injected into the dorsal region of mice, and changes in the volumes of the fillers were observed. Both HA and HA–PN fillers displayed an increase in volume for up to 4 weeks. The largest volume was observed for Juvéderm VOLUMA (250 mm<sup>3</sup>), followed by those for Juvéderm VOLBELLA (158 mm<sup>3</sup>), HA–PN 0.1%, 0.5% (134 mm<sup>3</sup>), and HA–PN 1% (127 mm<sup>3</sup>). These results suggested that the higher the concentration of HA, the larger is the volume growth rate. In addition, although the HA concentrations (1.5%) for Juvéderm VOLBELLA and the HA–PN complex filler were the same, the volume growth

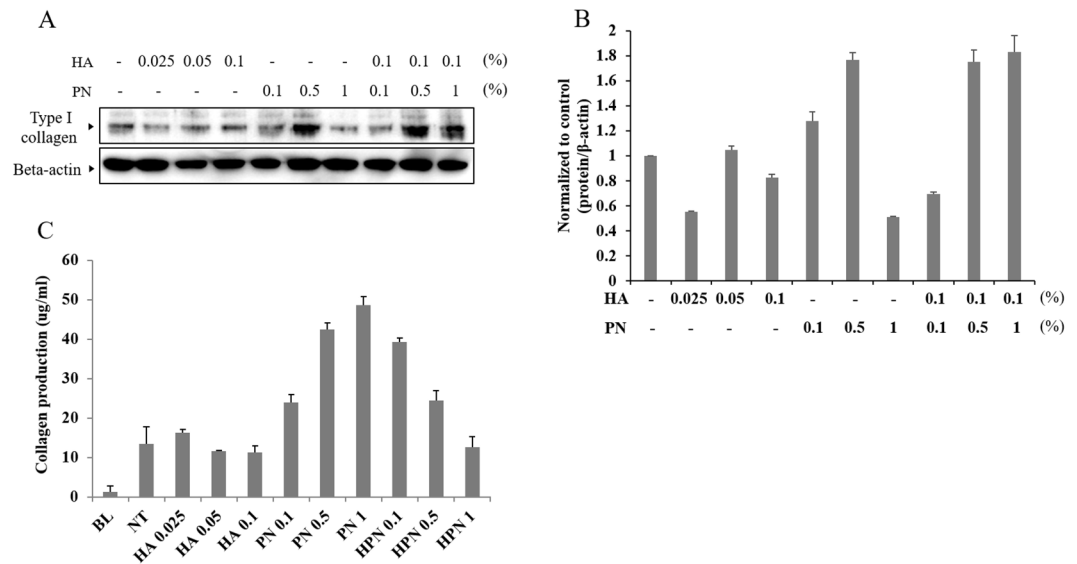


**Figure 4.** Quantification of the amount of type I collagen expressed in HDF cells. **(A)** Western blot image. **(B)** Quantification of the type I collagen expression in HDF cells. **(C)** Quantification of soluble collagen in the cell culture supernatant using Sircol collagen assay.

rate decreased in a dose-dependent manner for PN. Both injection fillers decreased in volume over time from 4 weeks after filler injection to 24 weeks of evaluation. The volume changes were as follows: Juvéderm VOLUMA, 120 mm<sup>3</sup>; Juvéderm VOLBELLA and HA–PN 0.5%, 98 mm<sup>3</sup>; HA–PN 0.1%, 92 mm<sup>3</sup>; HA–PN 1%, 97 mm<sup>3</sup> (Fig. 5).

**Comparison of histological analysis results between HA and HA–PN complex fillers.** To confirm the degree of inflammation and reaction with foreign bodies *in vivo*, skin tissue at the filler injection site was biopsied at 0 h, 12 weeks, and 24 weeks. Haematoxylin and eosin-stained tissue slides were observed at 100× magnification using an optical microscope, and the main histological features of each slide were determined. Histopathological evaluation showed that there was no reaction to foreign bodies upon the injection of both fillers (Fig. 6). However, with the 1% HA–PN complex filler, the presence of inflammatory cells was detected immediately following filler injection. No inflammatory cells were observed at week 12. Collagen synthesis was confirmed after staining with Masson’s trichrome. Thus, compared to the HA filler, the complex filler containing PN was associated with greater collagen synthesis.

**Comparison of transient receptor potential vanilloid 4 (TRPV4) expression between HA and HA–PN complex fillers by immunofluorescence analysis.** TRPV4 tissue staining was performed to determine the degree of stimulation in the tissue owing to filler injection. TRPV4 mediates pain-related behaviour caused by mild hyperactivity in the presence of inflammatory mediators. Immunofluorescence staining was confirmed at 4 weeks, and the maximum volume was measured after each filler injection. TRPV4 expression increased in the muscle layer after treatment with the HA fillers Juvéderm VOLUMA (2.0%) and Juvéderm VOLBELLA (1.5%). On the contrary, the TRPV4 expression level after HA–PN 1% complex filler treatment was equivalent to that for treatment with the negative control, PBS (Fig. 7).

## Discussion

The terms “biological stimulation” and “biological regeneration” have been used to describe the functions of many aesthetic medical devices<sup>22</sup>. Regeneration is the process of restoration and growth that makes the genome, cell, organism, and ecosystem resilient to events that cause natural fluctuations, disturbances, or damages<sup>23,24</sup>. Several clinical studies have described the therapeutic use of polynucleotides in skin regeneration and wound healing<sup>25–28</sup>. The HA–PN complex filler, composed of HA and PN polymer, is a new formulation for skin regeneration and tissue restoration. We confirmed the improved functions of the HA–PN complex filler through comparisons with the Juvéderm VOLUMA and Juvéderm VOLBELLA high-volume HA fillers. Moreover, we further analysed and compared all these fillers in terms of their morphological and rheological properties, and their effects in cells and animal models.

Polynucleotides are widely distributed in the human body and exist physiologically in the extracellular environment<sup>29</sup>. They readily bind to water molecules and act as free radical scavengers<sup>30,31</sup>. The nutritional effects of PN have been shown in multiple *in vitro* studies using human fibroblasts in primary cultures. The ability of PN to stimulate the secretion of collagen proteins and other proteins in the extracellular matrix has also been demonstrated<sup>32–34</sup>.

The HA–PN complex filler is morphologically similar to the HA filler. However, we confirmed that its rheological properties, in terms of  $G^*$ ,  $G'$ ,  $G''$ , and  $\tan \delta$ , are different from those of the HA filler. It was confirmed that the hardness, elasticity, viscosity, and viscoelasticity of the cross-linked gel are dependent on the PN content of the HA–PN complex filler. In addition, no toxicity was associated with PN or HA–PN treatments in human

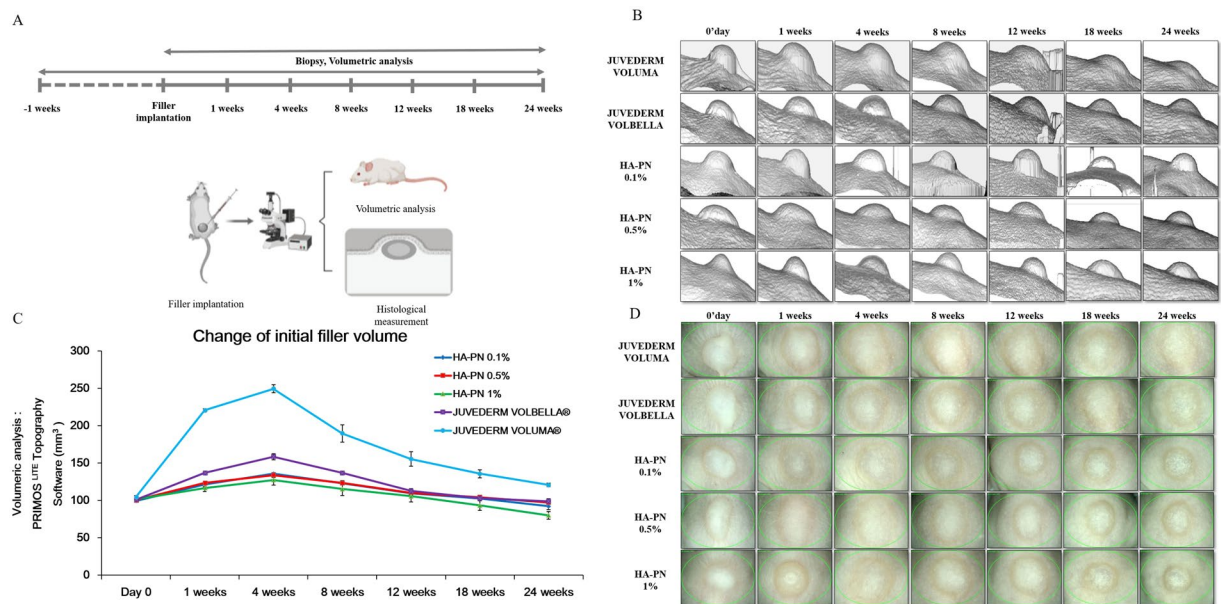


**Figure 5.** Evaluation of durability of HA and HA-PN complex fillers in vivo. (A) Study design scheme (Created with BioRender). (B) Image depicting volume change after the filler injection was taken using PRIMOS. (C) Graph showing volume change after filler injection. (D) A folliscope image depicting volume change after filler injection.

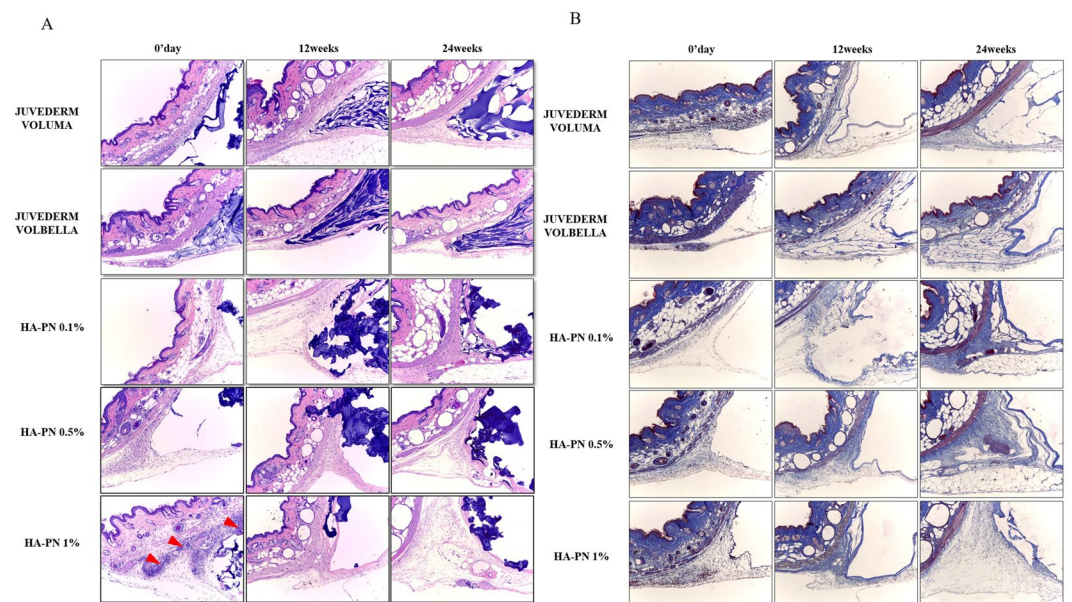


**Figure 6.** Histological evaluation of HA and HA-PN fillers. (A) Identification of inflammation and foreign body reaction by hematoxylin and eosin staining at Day 0, Week 12 and Week 24. (B) Identification of collagen production using Masson's trichrome staining at Day 0, Week 12 and Week 24.

and mouse fibroblast cells. Moreover, in human fibroblast cells, the content of type I collagen increased with the increasing PN concentration. However, excess PN inhibited the synthesis of type 1 collagen.

In animal studies, the HA-PN complex filler showed the greatest increase in collagen synthesis and maintained a natural volume, with no significant increases in the initial filler injection volume. In addition, previous studies have identified six TRPV proteins as receptors for stimulation of neurons<sup>35,36</sup>. Among these TRPV proteins, TRPV4 is a ubiquitously expressed plasma membrane-based calcium-permeable cation channel that is sensitised and activated by chemical and physical stimulation<sup>37–40</sup>. When skin is stimulated, the expression of matrix metalloproteinases (MMPs) and inflammatory cytokines can increase<sup>41,42</sup>. The increased levels of MMPs result in the degradation of collagen and elastic fibres in the skin and promote skin aging<sup>43,44</sup>. In this study, HA

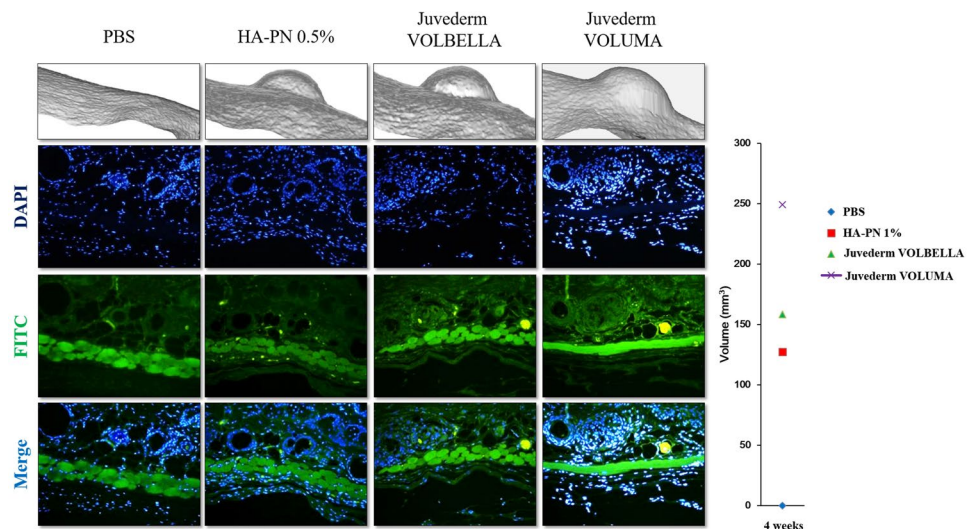


**Figure 7.** Comparison of TRPV4 expression after treatment with HA and HA–PN fillers using immunofluorescence staining of mouse tissue. The extent of stimulation in tissues by TRPV4 at Week 4 was determined using immunofluorescence staining. The increases in volume as a result of filler treatments were also compared.

filler containing PN induced a lower expression of the TRPV4 protein, a neuronal stimulatory receptor, compared to HA filler. When PN was included, it induced a reduced stimulation and lower MMP and inflammatory cytokine expression. This finding indicated that HA fillers containing PN are more effective in inhibiting skin aging compared to HA fillers. Numerous fillers have been developed and used to achieve simple volume effects. However, HA–PN complex fillers can stimulate fibroblast growth for skin rejuvenation and have the added benefits of volume enhancement and skin regeneration. In addition, the trend is currently shifting from the provision of components (such as collagen, HA, and glycoproteins) into the skin to the stimulation of cellular components (such as fibroblasts) to enhance regeneration. To the best of our knowledge, this is the first study demonstrating the durability, efficacy, and safety of HA–PN complex fillers. We believe that our results can potentially be the next-generation paradigm in the filler market.

## Methods

**Materials.** The HA–PN complex filler was supplied by NutraPharmTech (Seoul, Korea). It was prepared by mixing in the PN solution after sterilising the HA-based filler, which is generally cross-linked by BDDE. HA fillers made by Allergan were purchased from Juvéderm VOLUMA and Juvéderm VOLBELLA (Pringy, France). Type I collagen antibody (ab34710) and transient receptor potential vanilloid (TRPV4; ab39260) proteins were obtained from Abcam (Cambridge, Mass.).

**Scanning electron microscopy.** The morphology of each filler was evaluated using SEM. Each filler was diluted with water for injection (WFI), filtered through a 0.22  $\mu\text{m}$  membrane filter mounted in a stainless-steel filter housing, and then placed in an oven until the filter contents were completely dry. Filler samples were mounted on stainless steel SEM pedestals pre-labelled with double-sided adhesive mounting disks. Samples were prepared by coating with gold-palladium powder and conventionally imaged using a LEO SUPRA 55 microscope (Carl Zeiss, Jena, Germany).

**Rheological measurements.** The storage modulus ( $G'$ ) and viscous modulus ( $G''$ ) were measured using a rheometer (Kinexus Pro, Malvern, UK).  $G'$  characterises the stiffness of the gel – a stiff material has a higher  $G'$  than a soft material. All measurements were carried out using a 20-mm steel plate oscillating at a frequency between 0.1 and 10 Hz. The values presented were compared to the average of the values obtained at frequencies of 1 to 10 Hz. Measurement conditions were as follows: oscillation mode; a shear strain of 1.5%; a frequency of 0.05 to 25 Hz; an interval of 0.5 mm; and a temperature of 25  $^{\circ}\text{C}$ .

**Cell maintenance.** HDF cells (CCD-25SK; American Type Culture Collection, Manassas, VA, USA) were grown in Dulbecco's modified Eagle's medium (DMEM) Supplemented with 10% foetal bovine serum (FBS), 2 mM L-glutamine, 100 U/mL penicillin, and 100 mg/mL streptomycin, at 37  $^{\circ}\text{C}$  in a humidified incubator with a 5%  $\text{CO}_2$  atmosphere<sup>45</sup>. In addition, an established mouse fibroblast cell line (L929, catalogue code CCL-1; American Type Culture Collection) was cultured in minimal essential medium Supplemented with 5% foetal calf serum, 100 U/mL penicillin, 100  $\mu\text{L}/\text{mL}$  streptomycin, and 2 mmol/L L-glutamine at 37  $^{\circ}\text{C}$  in a humidified incubator with a 5%  $\text{CO}_2$  atmosphere<sup>46</sup>.

**Cell viability.** The MTT assay was performed to measure the cell viability of the HDFs and L929 mouse fibroblasts. HA (0.025% to 0.1%) and PN (0.1% to 1%) were added after 5 h of cell culture. MTT solution (5 mg/mL) was added and incubated at 37  $^{\circ}\text{C}$  for 4 h. After incubation, the supernatant was removed, and the formazan

formed by MTT reduction was dissolved in dimethylsulfoxide<sup>47</sup>. The absorbance of formazan was measured at 570 nm using a SoftMax Pro5 ELISA microplate reader (Molecular Devices, Sunnyvale, CA, USA).

**Wound healing assay for cell mobility.** The wound healing assay was performed based on previous studies by measuring cell migration. The cell migration is defined as the time taken to close an open wound after a linear 'scratch' or wound is created across a monolayer of cultured cells<sup>48,49</sup>.

Ibidi culture-inserts ( $\mu$ -Dish 35 mm, high culture-inserts; Thistle Scientific Ltd., Glasgow, UK) were used for the assay. The sample was diluted in DMEM and was used to treat the cells, which were then cultured for 24 to 72 h. DMEM Supplemented with 10% FBS was used as a positive control. After 48 h, the movement of cells was photographed using an Eclipse TS100 inverted microscope (Nikon Instruments Inc., Tokyo, Japan). Images were normalised using the XnConvert software and wound sites were quantified using the Image J software (ImageJ; version 1.51 i; U.S. National Institutes of Health). The final wound area was quantified and expressed as a percentage of the initial wound area. This represented the degree of wound healing at that point in time.

**Western blotting.** HDF cells were cultured in DMEM Supplemented with FBS for 24 h. The treated cells were exposed to different concentrations of HA and PN in the absence or presence of FBS. Every hour during the culture, the treated and control cells were collected and a defined amount of total protein, as determined using the Bradford protein assay (Bio-Rad Laboratories, Hercules, CA, USA), was resolved using 10% SDS-PAGE. The resolved proteins were transferred to a polyvinylidene fluoride membrane. After the application of primary antibodies and conjugated secondary antibodies, each membrane was washed thrice for 10 min with Tris-buffered saline containing 0.1% Tween 20. The degree of protein expression was determined using ECL detection reagents (Thermo Fisher Scientific, Pierce Biotechnology, Waltham, MA, USA).

**Collagen measurement.** The total soluble collagen from cell culture supernatants was quantified using the Sircol collagen assay, according to the manufacturer's instructions (Biocolor, Belfast, UK)<sup>50</sup>. The absorbance was then measured at 555 nm, as it is directly proportional to the amount of collagen present in the cell culture medium. The soluble collagen was then hydrolysed in HCl, and the hydroxyproline levels were measured by a colourimetric method using an assay kit (QuickZyme Biosciences, Burlington, NC, USA), according to the manufacturer's instructions<sup>51,52</sup>. The total collagen content was calculated from the hydroxyproline content of collagen standards<sup>50</sup>.

**Study design.** All animal procedures were performed in accordance with the Guidelines for the Care and Use of Laboratory Animals of Chung-Ang University and approved by the Animal Ethics Committee of Chung-Ang University IACUC (Approval No. 201700022). Six-week-old SKH1 hairless mice were bred under temperature cycles of  $24 \pm 2$  °C,  $50 \pm 10\%$  humidity, and 12 h day/night cycles in the laboratory. The filler (100  $\mu$ L) was injected into the dorsal skin of the posterior limbs of hairless female mice ( $n = 5$  mice per group).

**Volumetric analysis.** The volume of filler injected into each dorsal skin was measured in the anesthetised mice. After filler injection, the increase in volume was determined using a PRIMOS device at 0, 1, 4, 8, 12, 18, and 24 weeks. The volume ratios were calculated by comparing the volume and height measurements at each time point to the measurements on Day 0. The change in volume was quantitatively determined through three-dimensional (3D) measurements of the skin region at the different time points before and after treatment and computer-assisted comparison of the measured profile<sup>53</sup>.

**Histological analyses.** Paraffin-embedded tissue sections were deparaffinised and stained according to previously published protocols<sup>54</sup>. Skin samples were fixed in 10% phosphate-buffered formaldehyde, embedded in paraffin, and processed for histological analysis. Sections, 5  $\mu$ m in thickness, were sliced and mounted on slides. The sections were stained with haematoxylin and eosin (to confirm inflammation and foreign body reaction) and Masson's trichrome (to confirm collagen biosynthesis), according to standard procedures.

**Immunofluorescence analysis.** Paraffin-embedded tissue sections were deparaffinised and stained according to previously published protocols<sup>55</sup>. Anti-Transient Receptor Potential Cation Channel Subfamily V Member 4 (TRPV4) antibody (ab39260, 1:200; Abcam) was used as the primary antibody. After treatment with a blocking buffer containing 2.5% bovine serum albumin (BSA, Sigma-Aldrich, St. Louis, MO, USA) and 2.5% horse serum, the cells were incubated at 25 °C for 4 h. The tissues were washed with phosphate-buffered saline containing 0.1% Triton X-100 (PBST). A fluorescein isothiocyanate-goat anti-rabbit secondary antibody, which exhibits green fluorescence, was added to the blocking buffer containing 2.5% BSA and left in a dark room for 2 h.

**Statistical analyses.** Statistical significance was computed using SPSS version 21 software (SPSS Inc., Chicago, IL, USA). One-way ANOVA and two-tailed unpaired *t*-tests were performed. \* $p \leq 0.05$ , \*\* $p \leq 0.005$ , \*\*\* $p \leq 0.0005$ .

### Data availability

All data generated or analysed during this study are included in this published article and its Supplementary Information Files. Extra data are available from the corresponding author upon request.

Received: 6 November 2019; Accepted: 18 February 2020;

Published online: 20 March 2020

## References

- Kruglikov, I. L. & Wollina, U. Soft tissue fillers as non-specific modulators of adipogenesis: change of the paradigm? *Exp Dermatol* **24**, 912–915, <https://doi.org/10.1111/exd.12852> (2015).
- Wise, J. B. & Greco, T. Injectable treatments for the aging face. *Facial Plast Surg* **22**, 140–146, <https://doi.org/10.1055/s-2006-947720> (2006).
- Wu, D. C. *et al.* Evaluation of the *in vivo* effects of various laser, light, or ultrasound modalities on human skin treated with a collagen and polymethylmethacrylate microsphere dermal filler product. *Lasers Surg Med* **48**, 811–819, <https://doi.org/10.1002/lsm.22580> (2016).
- Wang, F. *et al.* *In vivo* stimulation of de novo collagen production caused by cross-linked hyaluronic acid dermal filler injections in photodamaged human skin. *Arch Dermatol* **143**, 155–163, <https://doi.org/10.1001/archderm.143.2.155> (2007).
- Fidalgo, J. *et al.* Detection of a new reaction by-product in BDDE cross-linked autoclaved hyaluronic acid hydrogels by LC-MS analysis. *Med Devices (Auckl)* **11**, 367–376, <https://doi.org/10.2147/MDER.S166999> (2018).
- Keizers, P. H. J. *et al.* A high crosslinking grade of hyaluronic acid found in a dermal filler causing adverse effects. *J Pharm Biomed Anal* **159**, 173–178, <https://doi.org/10.1016/j.jpba.2018.06.066> (2018).
- Fino, P., Toscani, M., Grippaudo, F. R., Giordan, N. & Scuderi, N. Randomized Double-Blind Controlled Study on the Safety and Efficacy of a Novel Injectable Cross-linked Hyaluronic Gel for the Correction of Moderate-to-Severe Nasolabial Wrinkles. *Aesthetic Plast Surg* **43**, 470–479, <https://doi.org/10.1007/s00266-018-1284-x> (2019).
- Shi, X. H. *et al.* Complications from Nasolabial Fold Injection of Calcium Hydroxylapatite for Facial Soft-Tissue Augmentation: A Systematic Review and Meta-Analysis. *Aesthet Surg J* **36**, 712–717, <https://doi.org/10.1093/asj/sjv206> (2016).
- Taylor, S. C., Burgess, C. M. & Callender, V. D. Safety of nonanimal stabilized hyaluronic acid dermal fillers in patients with skin of color: a randomized, evaluator-blinded comparative trial. *Dermatol Surg* **35**(Suppl 2), 1653–1660, <https://doi.org/10.1111/j.1524-4725.2009.01344.x> (2009).
- Yeom, J. *et al.* Effect of cross-linking reagents for hyaluronic acid hydrogel dermal fillers on tissue augmentation and regeneration. *Ivconjug Chem* **21**, 240–247, <https://doi.org/10.1021/bc9002647> (2010).
- Iverson, S. M. & Patel, R. M. Dermal filler-associated malar oedema: Treatment of a persistent adverse effect. *Orbit* **36**, 473–475, <https://doi.org/10.1080/01676830.2017.1337203> (2017).
- Tran, C., Carraux, P., Micheels, P., Kaya, G. & Salomon, D. *In vivo* bio-integration of three hyaluronic acid fillers in human skin: a histological study. *Dermatology* **228**, 47–54, <https://doi.org/10.1159/000354384> (2014).
- Vidic, M. & Bartenjev, I. An adverse reaction after hyaluronic acid filler application: a case report. *Acta Dermatovenerol Alp Pannonica Adriat* **27**, 165–167 (2018).
- Wollina, U. & Goldman, A. Dermal fillers: facts and controversies. *Clin Dermatol* **31**, 731–736, <https://doi.org/10.1016/j.clindermatol.2013.05.010> (2013).
- Park, K. Y., Seok, J., Rho, N. K., Kim, B. J. & Kim, M. N. Long-chain polynucleotide filler for skin rejuvenation: efficacy and complications in five patients. *Dermatol Ther* **29**, 37–40, <https://doi.org/10.1111/dth.12299> (2016).
- Spano, S. J., Ghilzon, R., Lam, D. K., Goldberg, M. B. & Tenenbaum, H. C. Subperiosteal Papilla Augmentation With a Non-Animal-Derived Hyaluronic Acid Overlay Technique. *Clin Adv Periodontics*, <https://doi.org/10.1002/cap.10075> (2019).
- Muratore, O. *et al.* A human placental polydeoxyribonucleotide (PDRN) may promote the growth of human corneal fibroblasts and iris pigment epithelial cells in primary culture. *New Microbiol* **26**, 13–26 (2003).
- Ichikawa, M. *et al.* Decreased UV sensitivity, mismatch repair activity and abnormal cell cycle checkpoints in skin cancer cell lines derived from UVB-irradiated XPA-deficient mice. *Mutat Res* **459**, 285–298 (2000).
- Wu, C. L. *et al.* Proteomic analysis of UVB-induced protein expression- and redox-dependent changes in skin fibroblasts using lysine- and cysteine-labeling two-dimensional difference gel electrophoresis. *J Proteomics* **75**, 1991–2014, <https://doi.org/10.1016/j.jprot.2011.12.038> (2012).
- Hekimi, S., Wang, Y. & Noe, A. Mitochondrial ROS and the Effectors of the Intrinsic Apoptotic Pathway in Aging Cells: The Discerning Killers! *Front Genet* **7**, 161, <https://doi.org/10.3389/fgene.2016.00161> (2016).
- Pak, C. S. *et al.* A phase III, randomized, double-blind, matched-pairs, active-controlled clinical trial and preclinical animal study to compare the durability, efficacy and safety between polynucleotide filler and hyaluronic acid filler in the correction of crow's feet: a new concept of regenerative filler. *J Korean Med Sci* **29**(Suppl 3), S201–209, <https://doi.org/10.3346/jkms.2014.29.S3.S201> (2014).
- Avantaggiato, A. *et al.* Radiofrequency treatments: what can we expect? *J Biol Regul Homeost Agents* **30**, 217–222 (2016).
- Einhorn, T. A. & Lee, C. A. Bone regeneration: new findings and potential clinical applications. *J Am Acad Orthop Surg* **9**, 157–165 (2001).
- Goetsch, S. C., Hawke, T. J., Gallardo, T. D., Richardson, J. A. & Garry, D. J. Transcriptional profiling and regulation of the extracellular matrix during muscle regeneration. *Physiol Genomics* **14**, 261–271, <https://doi.org/10.1152/physiolgenomics.00056.2003> (2003).
- Kim, J. K. & Chung, J. Y. Effectiveness of polydeoxyribonucleotide injection versus normal saline injection for treatment of chronic plantar fasciitis: a prospective randomised clinical trial. *Int Orthop* **39**, 1329–1334, <https://doi.org/10.1007/s00264-015-2772-0> (2015).
- Lazzarotto, M., Tomasello, E. M. & Caporossi, A. Clinical evaluation of corneal epithelialization after photorefractive keratectomy in patients treated with polydeoxyribonucleotide (PDRN) eye drops: a randomized, double-blind, placebo-controlled trial. *Eur J Ophthalmol* **14**, 284–289 (2004).
- Rubegni, P., De Aloe, G., Mazzatenta, C., Cattarini, L. & Fimiani, M. Clinical evaluation of the trophic effect of polydeoxyribonucleotide (PDRN) in patients undergoing skin explants. A Pilot Study. *Curr Med Res Opin* **17**, 128–131 (2001).
- Squadrito, F. *et al.* Pharmacological Activity and Clinical Use of PDRN. *Front Pharmacol* **8**, 224, <https://doi.org/10.3389/fphar.2017.00224> (2017).
- Quirin, E. A. *et al.* Development of sequence characterized amplified region (SCAR) primers for the detection of Phyto.5.2, a major QTL for resistance to *Phytophthora capsici* Leon. in pepper. *Theor Appl Genet* **110**, 605–612, <https://doi.org/10.1007/s00122-004-1874-7> (2005).
- Misiaszek, R., Crean, C., Geacintov, N. E. & Shafirovich, V. Combination of nitrogen dioxide radicals with 8-oxo-7,8-dihydroguanine and guanine radicals in DNA: oxidation and nitration end-products. *J Am Chem Soc* **127**, 2191–2200, <https://doi.org/10.1021/ja044390r> (2005).
- Gaidamakova, E. K., Neumann, R. D. & Panyutin, I. G. Site-specific strand breaks in RNA produced by (125)I radiodecay. *Nucleic Acids Res* **30**, 4960–4965, <https://doi.org/10.1093/nar/gkf622> (2002).
- Furochi, H. *et al.* Overexpression of osteoactivin protects skeletal muscle from severe degeneration caused by long-term denervation in mice. *J Med Invest* **54**, 248–254 (2007).
- Marin, M. P. *et al.* Vitamin A deficiency alters the structure and collagen IV composition of rat renal basement membranes. *J Nutr* **135**, 695–701, <https://doi.org/10.1093/jn/135.4.695> (2005).
- Weisse, K., Brandsch, C., Hirche, F., Eder, K. & Stangl, G. I. Lupin protein isolate and cysteine-supplemented casein reduce calcification of atherosclerotic lesions in apoE-deficient mice. *Br J Nutr* **103**, 180–188, <https://doi.org/10.1017/S0007114509991565> (2010).
- Jain, A. *et al.* TRP-channel-specific cutaneous eicosanoid release patterns. *Pain* **152**, 2765–2772, <https://doi.org/10.1016/j.pain.2011.08.025> (2011).

36. Ohsaki, A., Tanuma, S. I. & Tsukimoto, M. TRPV4 Channel-Regulated ATP Release Contributes to gamma-Irradiation-Induced Production of IL-6 and IL-8 in Epidermal Keratinocytes. *Biol Pharm Bull* **41**, 1620–1626, <https://doi.org/10.1248/bpb.b18-00361> (2018).
37. Everaerts, W., Nilius, B. & Owsianik, G. The vanilloid transient receptor potential channel TRPV4: from structure to disease. *Prog Biophys Mol Biol* **103**, 2–17, <https://doi.org/10.1016/j.pbiomolbio.2009.10.002> (2010).
38. Gao, X., Wu, L. & O'Neil, R. G. Temperature-modulated diversity of TRPV4 channel gating: activation by physical stresses and phorbol ester derivatives through protein kinase C-dependent and -independent pathways. *J Biol Chem* **278**, 27129–27137, <https://doi.org/10.1074/jbc.M302517200> (2003).
39. Montell, C., Birnbaumer, L. & Flockerzi, V. The TRP channels, a remarkably functional family. *Cell* **108**, 595–598, [https://doi.org/10.1016/s0092-8674\(02\)00670-0](https://doi.org/10.1016/s0092-8674(02)00670-0) (2002).
40. Vriens, J. *et al.* Cell swelling, heat, and chemical agonists use distinct pathways for the activation of the cation channel TRPV4. *Proc Natl Acad Sci USA* **101**, 396–401, <https://doi.org/10.1073/pnas.0303329101> (2004).
41. Bauge, C., Leclercq, S., Conrozier, T. & Boumediene, K. TOL19-001 reduces inflammation and MMP expression in monolayer cultures of tendon cells. *BMC Complement Altern Med* **15**, 217, <https://doi.org/10.1186/s12906-015-0748-7> (2015).
42. Di Girolamo, N., Lloyd, A., McCluskey, P., Filipic, M. & Wakefield, D. Increased expression of matrix metalloproteinases *in vivo* in scleritis tissue and *in vitro* in cultured human scleral fibroblasts. *Am J Pathol* **150**, 653–666 (1997).
43. Huang, C. H. *et al.* Hinokitiol Exerts Anticancer Activity through Downregulation of MMPs 9/2 and Enhancement of Catalase and SOD Enzymes: *In Vivo* Augmentation of Lung Histoarchitecture. *Molecules* **20**, 17720–17734, <https://doi.org/10.3390/molecules201017720> (2015).
44. Im, A. R., Nam, K. W., Hyun, J. W. & Chae, S. Phloroglucinol Reduces Photodamage in Hairless Mice via Matrix Metalloproteinase Activity Through MAPK Pathway. *Photochem Photobiol* **92**, 173–179, <https://doi.org/10.1111/php.12549> (2016).
45. Biswas, M., Kwong, E. K., Park, E., Nagra, P. & Chan, J. Y. Glycogen synthase kinase 3 regulates expression of nuclear factor-erythroid-2 related transcription factor-1 (Nrf1) and inhibits pro-survival function of Nrf1. *Exp Cell Res* **319**, 1922–1931, <https://doi.org/10.1016/j.yexcr.2013.04.013> (2013).
46. Kumar, H. *et al.* Safety and tolerability of intradiscal implantation of combined autologous adipose-derived mesenchymal stem cells and hyaluronic acid in patients with chronic discogenic low back pain: 1-year follow-up of a phase I study. *Stem Cell Res Ther* **8**, 262, <https://doi.org/10.1186/s13287-017-0710-3> (2017).
47. Gasparini, L. S. *et al.* *In vitro* Cell Viability by CellProfiler(R) Software as Equivalent to MTT Assay. *Pharmacogn Mag* **13**, S365–S369, <https://doi.org/10.4103/0973-1296.210176> (2017).
48. Justus, C. R., Leffler, N., Ruiz-Echevarria, M. & Yang, L. V. *In vitro* cell migration and invasion assays. *J Vis Exp*, <https://doi.org/10.3791/51046> (2014).
49. Liang, C. C., Park, A. Y. & Guan, J. L. *In vitro* scratch assay: a convenient and inexpensive method for analysis of cell migration *in vitro*. *Nat Protoc* **2**, 329–333, <https://doi.org/10.1038/nprot.2007.30> (2007).
50. Lareu, R. R., Zeugolis, D. I., Abu-Rub, M., Pandit, A. & Raghunath, M. Essential modification of the Sircol Collagen Assay for the accurate quantification of collagen content in complex protein solutions. *Acta Biomater* **6**, 3146–3151, <https://doi.org/10.1016/j.actbio.2010.02.004> (2010).
51. Palko, J. R. *et al.* Biomechanical properties and correlation with collagen solubility profile in the posterior sclera of canine eyes with an ADAMTS10 mutation. *Invest Ophthalmol Vis Sci* **54**, 2685–2695, <https://doi.org/10.1167/iovs.12-10621> (2013).
52. Samuel, C. S. Determination of collagen content, concentration, and sub-types in kidney tissue. *Methods Mol Biol* **466**, 223–235, [https://doi.org/10.1007/978-1-59745-352-3\\_16](https://doi.org/10.1007/978-1-59745-352-3_16) (2009).
53. Kim, J. S., In, C. H., Park, N. J., Kim, B. J. & Yoon, H. S. Comparative study of rheological properties and preclinical data of porous polycaprolactone microsphere dermal fillers. *J Cosmet Dermatol*, <https://doi.org/10.1111/jocd.13076> (2019).
54. Yamashina, M., Takami, T., Kanemura, T., Orii, T. & Ojima, A. Immunohistochemical demonstration of complement components in formalin-fixed and paraffin-embedded renal tissues. *Lab Invest* **60**, 311–316 (1989).
55. Skilbeck, N. W. Immunofluorescent staining of leptospines in pepsin treated histologic sections. *Stain Technol* **61**, 273–278, <https://doi.org/10.3109/10520298609109953> (1986).

## Author contributions

Beom Joon Kim, Jong Hwan Kim and Tae-Rin Kwon designed research. Sung Eun Lee, Yoo Na Jang and Jong Hwan Kim performed research. Tae-Rin Kwon, Hye Sung Han and Beom Joon Kim analyzed data. Seog Kyun Mun, Tae-Rin Kwon, Jong Hwan Kim and Beom Joon Kim interpreted data. Jong Hwan Kim, Tae-Rin Kwon and Beom Joon Kim wrote the paper. All authors reviewed the manuscript.

## Competing interests

The authors declare no competing interests.

## Additional information

**Supplementary information** is available for this paper at <https://doi.org/10.1038/s41598-020-61952-w>.

**Correspondence** and requests for materials should be addressed to B.J.K.

**Reprints and permissions information** is available at [www.nature.com/reprints](http://www.nature.com/reprints).

**Publisher's note** Springer Nature remains neutral with regard to jurisdictional claims in published maps and institutional affiliations.



**Open Access** This article is licensed under a Creative Commons Attribution 4.0 International License, which permits use, sharing, adaptation, distribution and reproduction in any medium or format, as long as you give appropriate credit to the original author(s) and the source, provide a link to the Creative Commons license, and indicate if changes were made. The images or other third party material in this article are included in the article's Creative Commons license, unless indicated otherwise in a credit line to the material. If material is not included in the article's Creative Commons license and your intended use is not permitted by statutory regulation or exceeds the permitted use, you will need to obtain permission directly from the copyright holder. To view a copy of this license, visit <http://creativecommons.org/licenses/by/4.0/>.

© The Author(s) 2020